Synthesis of nanostructured AlN by solid state reaction of Al and diaminomaleonitrile

S.A. Rounaghi [a,b,*], H. Eshghi [c], A.R. Kiani Rashid [a], J. Vahdati Khaki [a], M. Samadi Khoshkhoo [b], S. Scudino [b], J. Eckert [b,d]

[a] Department of Materials Engineering, Ferdowsi University of Mashhad. P.O. Box no. 91775-1111, Mashhad, Iran
[b] IFW Dresden, Institut für Komplexe Materialien, Postfach 27 01 16, Dresden D-01171, Germany
[c] Department of Chemistry, Ferdowsi University of Mashhad. P.O. Box no. 91775-1436, Mashhad, Iran
[d] TU Dresden, Institut für Werkstoffwissenschaft, Dresden D-01062, Germany

ARTICLE INFO

ABSTRACT

The solid state reaction of diaminomaleonitrile (DAMN) with aluminum via both mechanochemical and thermal treatment routes was studied by X-ray diffraction and Fourier transform infrared spectroscopy. During the milling process, the reaction starts with the deammoniation of the DAMN molecules, followed by the formation of nanostructured AlN powder as the main solid product after milling for 7 h. The reactivity of the mixed powder was also investigated during the conventional thermal treatment process using differential scanning calorimetry, derivative thermogravimetry and thermogravimetric analysis. The results reveal that DAMN starts to polymerize at 192 °C by the elimination of the amine groups. Furthermore, increasing the annealing temperature leads to the formation of a nitrogen-containing carbonaceous material with the structure similar to non-crystalline carbon. However, no evidence for the formation of AlN was observed in the annealed samples even at temperatures as high as the Al melting point.

1. Introduction

Metal nitrides are a wide group of ceramic materials with individual properties and extensive industrial applications. Among the others, group III-nitrides present a large potential for applications in optoelectronic devices [1,2]. One of the group III-nitrides which attracted much attention during recent two decades is the aluminum nitride. Some unique features, such as high thermal conductivity, low dielectric constant, low linear thermal expansion coefficient and large band gap (6.2 eV), make AlN a potential candidate for electronic industrial applications like electronic packages, heat sinks and optical devices [3–6].

AlN can be synthesized by a variety of techniques, such as carbothermal reduction [6], direct nitridation process [7,8], chemical vapor deposition (CVD) [9,10], metalorganic chemical vapor deposition (MOCVD) [11], organometallic procedure [12], solvothermal process [13], combustion synthesis [14] and mechanochemical synthesis [15,16]. Among these methods, mechanochemical synthesis through ball milling stands out as the easiest way for the fabrication of nitrides without requiring

any controlled atmosphere condition and high technological equipment [17]. Milling can also be used as a pre-treatment step, namely "mechanical-activation", for other synthesizing methods, especially when a significant reduction in reaction temperature is desirable [18,19].

Most of the research on mechanochemical synthesis of AlN have been performed by the solid–gas metathesis (SGM) route, which consists of the reactive milling of Al or Al_2O_3 under N_2 or NH_3 atmosphere [15,16]. Yet, the full conversion of the reactants into AlN can hardly be achieved in a reasonable time due to the high stability of N_2 and the poor contacting of the reactant materials (solid–gas). Moreover, in most cases, processing in a controlled atmosphere is also required. In order to overcome these limitations, the gaseous nitrogen-rich phase should be substituted with solid nitrogen-containing (SNC) compounds to improve the contact between reactants and to promote the formation of the nitride product [20].

Recently, it has been demonstrated that organic SNC compounds can be used for synthesizing metal nitrides by the solid state metathesis (SSM) route. Based on this procedure, various metal oxides were heated in the presence of cyanamide [21] or one of its oligomers, such as disyanamide [22], melamine [23] and carbon nitride (C_3N_4) [24], in sealed conditions. As a result, the formation of a wide variety of metal nitride nanoparticles, such as AlN, GaN, VN and TiN, was reported using this processing route.

* Corresponding author at: Department of Materials Engineering, Ferdowsi University of Mashhad, Mashhad, Iran. Fax: +985118763305.
E-mail addresses: s.a.rounaghi@gmail.com, s.a.rounaghi@ifw-dresden.de (S.A. Rounaghi), heshghi@ferdowsi.um.ac.ir (H. Eshghi).
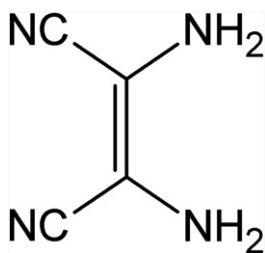
Fig. 1. Chemical structure of the DAMN molecule.

However, the high temperature required for the reaction completion (about 1150 °C in the case of AlN [21–23]) represents a serious drawback. Hence, there is the need for the reduction of the reaction temperature and for performing the tests in ambient atmosphere. To achieve these purposes, high-energy ball milling can be used as an alternative technique to the conventional thermal treatment processing. With regard to this, Zhang et al. introduced a milling procedure for synthesizing AlN by mechanochemical reaction of Al and melamine [25]. They successfully synthesized nanocrystalline AlN just after 14 h of milling at room temperature. Recently, we reported a mechanistic approach for the reaction which takes place during this milling process [26]. However, the specific symmetry of melamine s-triazine ring makes the mechanism difficult to be fully interpreted.

In this work, we developed a simple mechanochemical process for synthesizing AlN using a tetramer of cyanogen, the diaminomaleonitrile (DAMN), as a source of nitrogen. In contrast to cyanamide, cyanogen and its oligomers have not been used for formation of nitrides yet. DAMN is a low-cost organic compound with a high nitrogen content (the chemical structure of the DAMN molecule is illustrated in Fig. 1). The specific chemical geometry of nitrogen bonding in the DAMN molecule makes it more favorable than melamine or other materials with s-triazine rings from the viewpoint of chemical bond evolutions and may permit to follow the degradation and polymerization of the molecule during both mechanochemical and thermal treatment methods.

2. Experimental procedure

Al powder (purity 99.5%, Mashhad Powder Metallurgy Co.) was mixed with diaminomaleonitrile (purity 98%, Fluka) with a molar ratio of 4:1. The mixed powder (1.5 g) was charged into a steel vial together with stainless steel balls of two different sizes (10 and 8 mm) to give a ball to powder weight ratio of 50:1. After sealing the vial valve, milling process was conducted using a planetary ball-mill (manufactured by Khorasan Co.) in ambient atmosphere with rotating speed of 300 rpm for various times up to 12 h. Thermal analysis was carried out using a Netzsch 409 PC Luxx calorimeter at a heating rate of 10 °C/min under argon atmosphere. Phase analysis of the samples was performed by X-ray diffraction (XRD) using a Philips X'Pert X-ray diffractometer with CuKα radiation ($\lambda = 0.154060$ nm). In order to measure crystallite size of the milled products, the Rietveld method was used and the diffraction data were collected over a 2θ range of 4°–90° with a step width of 0.02°. Fourier transform infrared spectroscopy (FTIR) spectra were recorded using a ThermoNicolet Avatar 370 infrared spectrometer at room temperature with the KBr pellet technique. The measurements were obtained in the range 400–4000 cm^{-1} at a resolution of 2 cm^{-1}. Scanning electron microscopy (SEM) investigations were conducted using a Gemini 1530 (Zeiss) microscope operating at 20 kV.

High resolution transmission electron microscopy (HRTEM) investigations were performed using a Tecnai F30 (FEI company) microscope, operating at 300 kV. Samples were prepared by sonication of the powder in ethanol and putting a drop of suspension on a copper grid.

3. Results and discussion

3.1. Mechanochemical process

3.1.1. XRD analysis
Fig. 2 illustrates the phase evolution of the powder mixture during the milling process. The starting material (0 h) consists of a mixture of Al and DAMN. After milling for 6 h, the XRD pattern shows a significant broadening of the diffraction peaks belonging to Al and DAMN, which can be ascribed to grain refinement and to the introduction of lattice defects. No trace of AlN is detectable at this stage. Along with additional peak broadening for the Al and DAMN phases, the pattern of the powder mixture milled for 7 h reveals the presence of broad AlN diffraction peaks with very low intensity. With further milling up to 12 h, the peaks of the Al and DAMN reactants are no longer visible, whereas the intensity of the AlN peaks is remarkably increased, which indicates that the mechanochemical reaction is complete at this milling stage. The AlN XRD peaks are rather broad, which implies the formation of a nanocrystalline AlN structure. This is corroborated by Rietveld structure refinement, which reveals a mean crystallite size of about 18 nm for the AlN powder milled for 12 h.

3.1.2. FTIR characterization
The FTIR spectra for the powder mixture after different milling times are shown in Fig. 3. In order to identify possible bond changes occurring during milling, the IR spectrum of the pure as-received DAMN is also plotted in Fig. 3 (0 h). The main band characteristics of the DAMN arise from several functional groups; the bands obtained at 3200–3450 cm^{-1} correspond to the stretching vibration mode of the amine groups. The strong and sharp bands at 2166 and 2213 cm^{-1} are due to the stretching vibration mode of the nitrile groups. Other transmittance peaks at 1600–1650 cm^{-1}, 1200–1400 cm^{-1} and below 750 cm^{-1} result from the C=C and C–N bond stretching and the C–C bending and rotational vibrations, respectively.
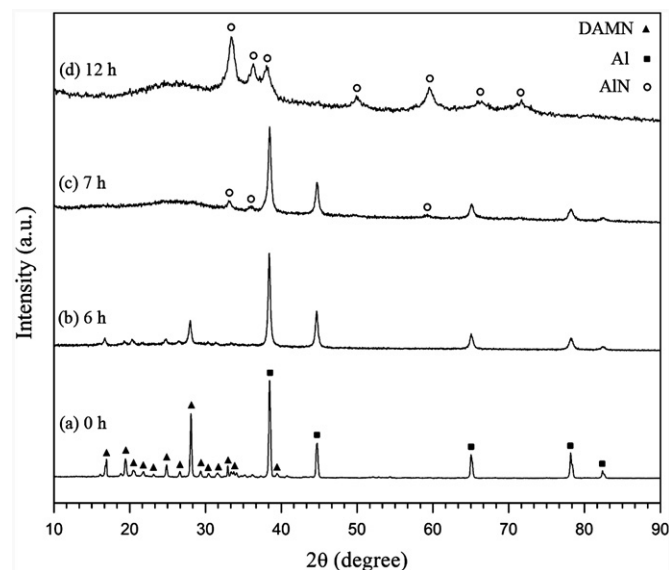

Fig. 2. XRD patterns of the powder mixture after milling for various times.
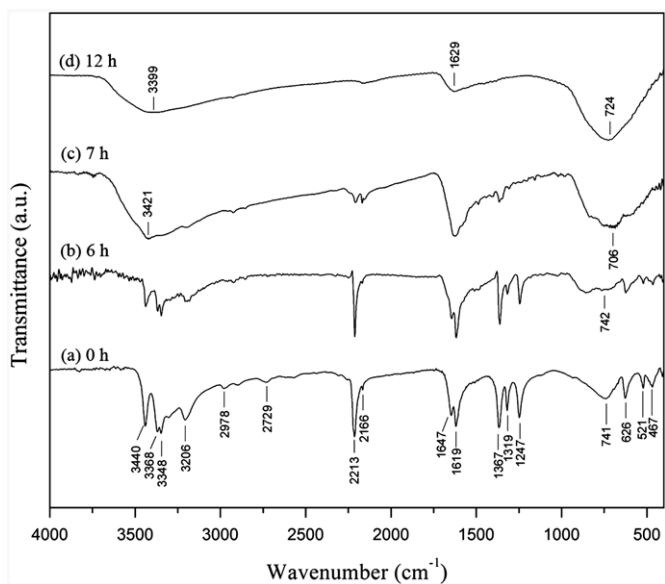
Fig. 3. FTIR spectra of the as-received pure DAMN (a) 0 h and of the powder mixture milled for (b) 6 h (c) 7 h and (d) 12 h.

In agreement with the XRD results (Fig. 2b), the IR spectrum of the powder milled for 6 h reveals that there are no visible changes in band characteristics and peak frequencies, confirming that no reaction takes place at this milling stage. Nevertheless, the characteristic pungent smell of ammonia was detected after opening the vial valve, indicating that partial deammoniation of DAMN occurs at this stage. It should be noted that the $-NH_2$ bonds are the weakest in the DAMN molecule (bond energy 276 kJ/mol). Therefore, it can be assumed that the $-NH_2$ bonds will be the first broken bonds during the milling process. This hypothesis is corroborated by the decrease of the $-NH_2$ band intensities in the relevant IR spectrum (Fig. 3b).

The partial deammoniation makes the DAMN molecule unstable and susceptible to further degradation. Therefore, fresh and activated Al particles can react with the unstable DAMN molecule to form AlN, which is thermodynamically more stable than other Al derivatives (such as aluminum carbide and hydride). With increasing the milling time up to 7 h, the Al particles preferably react with nitrogen of the DAMN molecule, which leads to the disappearance of the strong bands associated with the amine and nitrile groups in the IR spectrum (Fig. 3c). These significant changes of the band characteristics occur in the same milling stage when the formation of AlN is detected (Fig. 2c). The IR spectrum of AlN displays a characteristic transmittance band between 680 and 800 cm^{-1} corresponding to the Al–N stretching vibration mode [27]. This suggests that the transmittance peaks visible at 706 and 724 cm^{-1} related to the powder milled for 7 and 12 h, respectively (Fig. 3c and d) belong to the formation of AlN. Other broad peaks at 1629 cm^{-1} and about 3400 cm^{-1} can be associated to O–H bonds resulting from the moisture absorption on the surface of the powder [28].

3.1.3. SEM and TEM observations

SEM and HRTEM were used in order to analyze structure and morphology of the as-milled products. Fig. 4a shows the morphology of the powder particles milled for 12 h and the corresponding particle size distribution is displayed in Fig. 4b. The particles have irregular shape with average size smaller than 1 μm. The possible formation of nanoparticle (size < 100 nm) was investigated by TEM. Fig. 5a displays a typical HRTEM micrograph
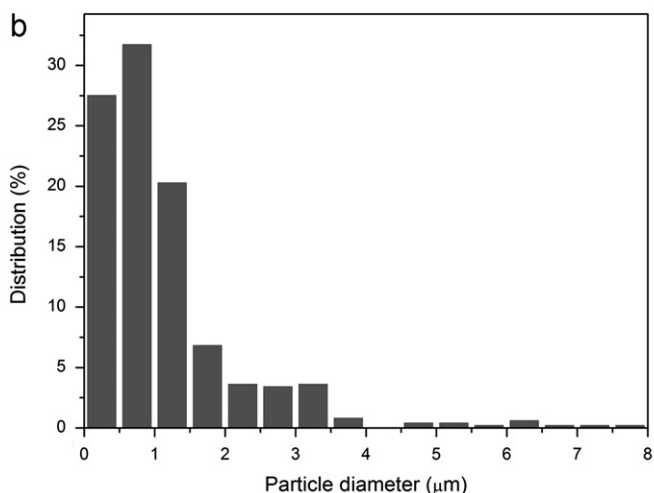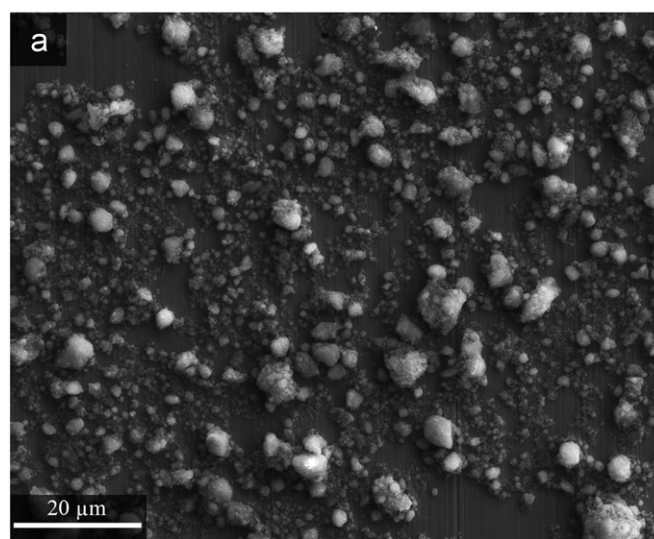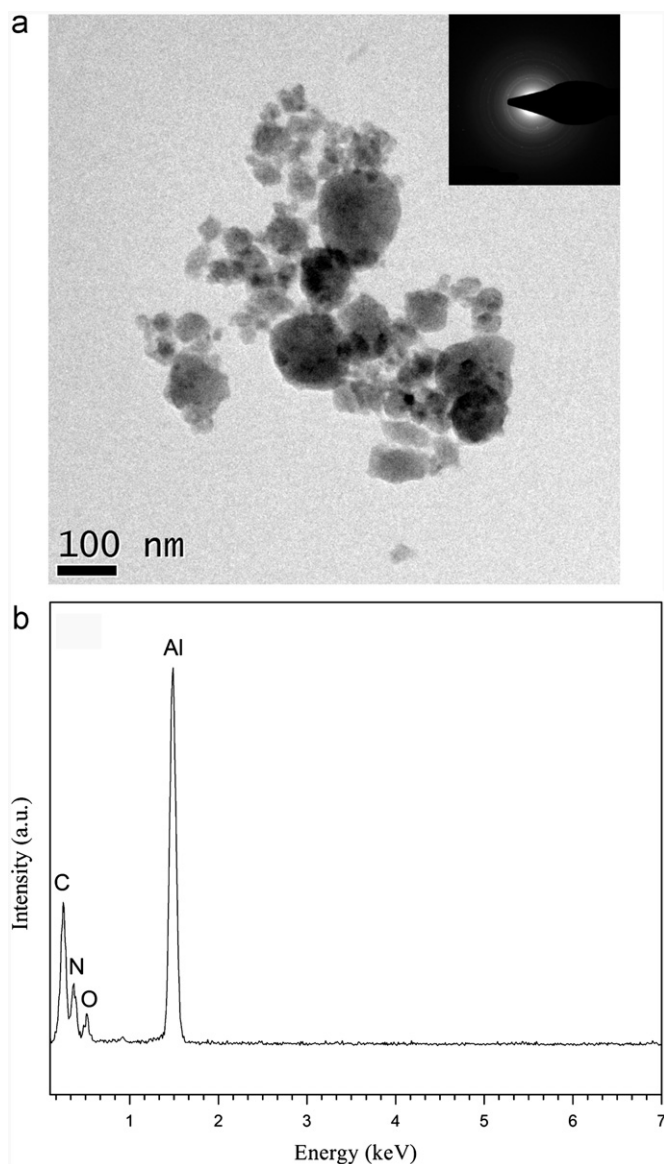

Fig. 4. (a) SEM image of the powder mixture milled for 12 h. (b) Particle size distribution histogram of the same sample.

of these fine particles. The corresponding selected area diffraction pattern (inset in Fig. 5a) reveals a perfect match of the substance with the h-AlN structure. Most of the particles have size smaller than 100 nm. This result indicates that the milling process not only leads to the formation of nanocrystalline AlN but also that some particles are in the nanometric size range. The chemical composition of the material was measured by energy-dispersive X-ray spectroscopy (EDS) and the result is shown in Fig. 5b. The EDS spectrum shows Al and N peaks corresponding to the AlN phase along with a C peak caused by residual carbon remaining after decomposition of the DAMN. An O peak resulting from oxygen contamination during handling and TEM sample preparation is also visible. It should be noted that the enthalpy of Al_2O_3 is higher than AlN and a layer of aluminum oxide can always be found on the surface of aluminum nitride particles [29,30].

3.2. Thermal treatment process

3.2.1. Thermal analysis

The possible solid state reaction between Al and DAMN induced by conventional thermal treatment was also investigated (Fig. 6a and b). Isochronal differential scanning calorimetry (DSC) reveals three distinct peaks: two endothermic peaks at 186 and 654 °C, and an exothermic peak at 194 °C (Fig. 6a). On the other hand, only the peak at 192 °C was recorded by derivative
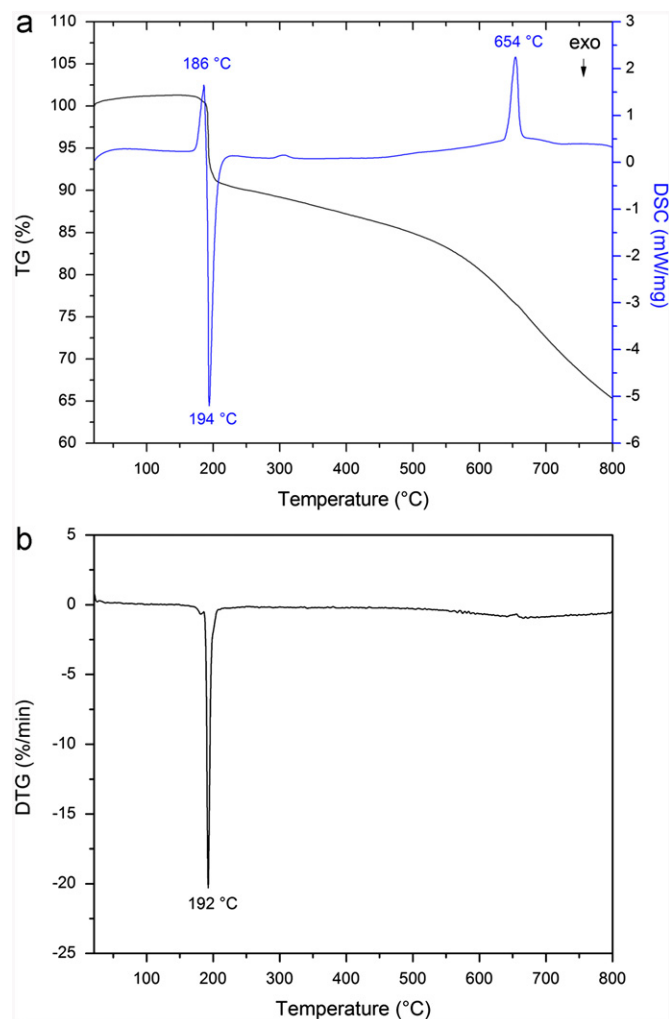
Fig. 5. (a) TEM image of the powder mixture milled for 12 h and (inset) corresponding electron diffraction pattern. (b) EDS spectrum of the same sample.

Fig. 6. (a) DSC and TG curves of the mixed powder isochronally heated under argon atmosphere. (b) DTG curve of the same sample.
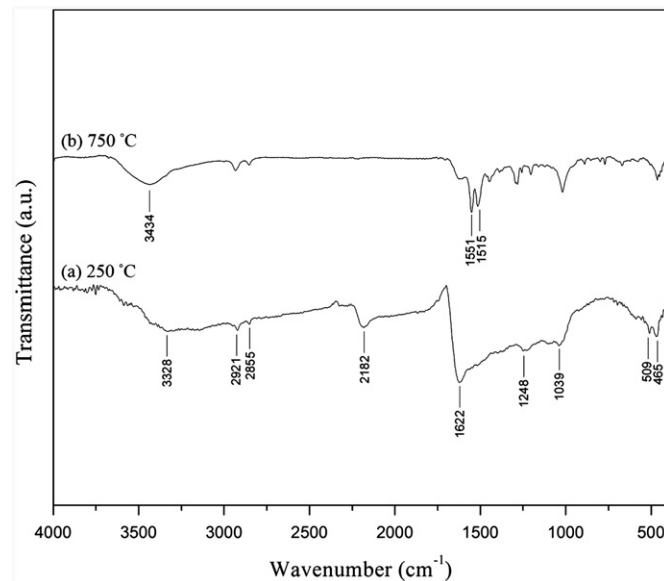
thermogravimetry (DTG) (Fig. 6b). These results suggest that the peak occurring at temperatures in the range of 192–194 °C can be associated with a phase transformation. In contrast, the peaks at 186 and 654 °C can be ascribed to melting of DAMN and Al, respectively, which cannot be detected by DTG analysis. In order to clarify the physical and chemical transformations occurring during heating, two samples were prepared by heating the mixed powder up to 250 and 750 °C, respectively (i.e. above the main peaks recorded by DSC) and by annealing them at these temperatures for 30 min under a continuous argon flux. Afterward, the annealed samples were cooled to ambient temperature and FTIR and XRD analysis of each sample was performed, as it will be presented in the following sections.

3.2.2. FTIR characterizations

FTIR spectra of the powder annealed for 30 min at different temperatures are shown in Fig. 7. Compared with as-received DAMN (Fig. 3a), a significant reduction of the band intensities at 3200–3450 cm^{-1} can be observed in the IR spectrum of the sample annealed at 250 °C (Fig. 7a). This behavior can be ascribed

Fig. 7. FTIR spectra of the powder annealed for 30 min at different temperatures: (a) 250 °C and (b) 750 °C.

to the dissociation of the DAMN and to the elimination of amine groups, indicating that, as observed during the milling process (Fig. 3), these bonds are the first to be broken during the thermal treatment. The removal of the $-NH_2$ bonds makes the molecule susceptible to further condensation by elimination of nitrile groups. Therefore, the conspicuous reduction of the $-C\equiv N$ bond intensities and the appearance of a broad transmittance peak in the range of 1000–1650 cm^{-1} (Fig. 7a) can be attributed to the polymerization of nitrile groups and to the formation of nitrogen-containing carbonaceous material with C/N aromatic ring structure, respectively [31–33]. Considering this fact, the abrupt weight loss observed in the TG and DTG thermographs at about 192 °C can be attributed to the elimination of amine groups as well as to the polymerization of the DAMN (Fig. 6a and b).

The IR spectrum in Fig. 7b reveals that the nitrile and amine transmittance bands are absent in the sample annealed at 750 °C. This indicates that a fully polymerized structure has been achieved at this temperature. A significant reduction of the band intensity of the aromatic C/N ring can also be observed, which can be attributed to the elimination of pyridinic nitrogen from the ring at high temperatures [31]. Indeed, in heterocyclic carbon materials, nitrogen plays an essential role in breaking the symmetry of carbon structure, making the structure IR active [34]. Hence, the elimination of nitrogen reduces the IR activity of the residual material. Nitrogen loss of the carbonaceous material is supported by the slight and continuous weight loss in the TG curve at high temperatures (Fig. 6a). Surprisingly, although C–N and C=N bonds of the ring start to break down at high temperatures, no evidence for the reaction of Al with the available nitrogen-rich species or with the remaining carbonaceous material is visible in Fig. 7a and b.

3.2.3. XRD analysis

Fig. 8a and b show the XRD patterns of the samples annealed for 30 min at 250 and 750 °C, respectively. No peaks corresponding to AlN are visible in the patterns, in agreement with the results obtained from IR and thermal analysis (Figs. 6 and 7). In addition, an extremely broad diffraction peak at 2θ between 24° and 30° can be observed after annealing at 250 °C (Fig. 8a).

This peak does not correspond to the as-received DAMN, which displays the strongest peak at $2\theta=28.05°$ (as illustrated in Fig. 2a), and it can be attributed to the polymerization of the DAMN. The broad diffraction peak becomes broader and it is shifted to lower angles after annealing at 750 °C (Fig. 8c). Most likely, this is due to the micro-structural evolution of the C/N material. At higher temperatures, the nitrogen content of the polymerized C/N material decreases significantly and the remaining material is believed to have a structure very similar to the non-crystalline carbon [31,32]. Hence, it can be concluded that the XRD peak is shifted to the position of the (002) diffraction peak of carbon (dotted line in Fig. 8c) as a result of the elimination of nitrogen at higher temperatures.
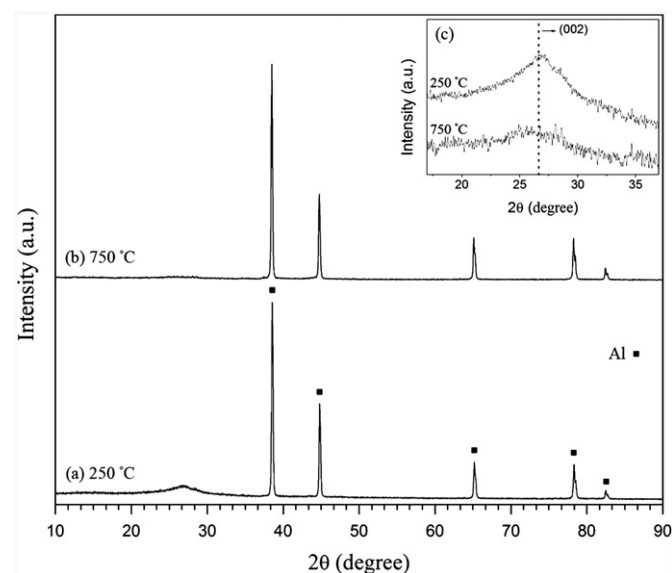
The present results indicate that high-energy milling makes the formation of nanostructured AlN possible even at room temperature. Moreover, the reaction occurs by solid state metathesis without the need of any controlled atmospheres. In contrast, no reaction was observed between the raw materials by heating the mixed powder in argon atmosphere at temperatures up to 800 °C. This is in contrast to the findings of other authors, who reported the formation of AlN by heating a mixture of alumina and SNC compounds [21–23]. This discrepancy is probably due to the different experimental conditions used. While in the present investigation annealing of the powder mixture was carried out under a continuous argon flux, previous investigations [21–23] were performed in sealed tubes or under isolated conditions. Nitrogen-containing atomic species (such as CN^+ and $CNHN^+$), which are produced during the pyrolysis of SNC compounds, are believed to play a crucial role in the reduction of metal oxide and in the formation of the nitride at high temperatures. Although the same active radicals can be produced during the polymerization of DAMN, gas removal from the system due to the argon flux may inhibit the reaction of these species with Al at elevated temperatures. The residual C/N material exhibits a high stability without any tendency to react with the Al particles even at temperatures as high as the Al melting point. Nonetheless, a liquid–solid metathesis reaction can still be expected especially at higher temperatures, where the molten Al particles can react with the remaining carbon-rich material to form aluminum carbide [35].

4. Conclusions

In summary, the mechanochemical reaction of Al and DAMN resulted in the formation of nanostructured AlN at room temperature. Partial deammoniation of DAMN occurs in the first stages of milling. This step makes the DAMN molecules unstable and susceptible to further degradation. With increasing the milling time, the unstable DAMN molecules lose the nitrile and amine functional groups. The formation of the AlN starts at this stage, as demonstrated by the Al–N bond recorded at 706 cm^{-1} in the relevant IR spectrum. In contrast, polymerization of DAMN was observed during the heat treatment process at 194 °C and was followed by the formation of C/N material with a structure similar to non-crystalline carbon. No reaction between Al and DAMN to form AlN was detected for annealing temperatures up to 750 °C. These outcomes indicate that mechanochemical processing through ball milling offers a large potential for an efficient and cost-effective production of nitrides.

Fig. 8. XRD patterns of the powder annealed for 30 min at different temperatures: (a) 250 °C, (b) 750 °C and (c) XRD patterns of the same specimens in the range between 20° and 35° (the dotted line refers to the (002) diffraction peak of carbon).

References

[1] M.A. Khan, M. Shatalov, H.P. Maruska, H.M. Wang, E. Kuokstis, Jpn. J. Appl. Phys. 44 (2005) 7191–7206.
[2] M.T. Hardy, D.F. Feezell, S.P. DenBaars, S. Nakamura, Mater. Today 14 (2011) 408–415.

[3] W.M. Yim, E.J. Stofko, P.J. Zanzucchi, J.I. Pankove, M. Ettenberg, S.L. Gilbert, J. Appl. Phys. 44 (1973) 292–296.
[4] Y. Taniyasu, M. Kasu, T. Makimoto, Nature 441 (2006) 325–328.
[5] Y. Baik, R.A.L. Drew, Key Eng. Mater. 122–124 (1996) 553–570.
[6] T. Ide, K. Komeya, T. Meguro, J. Tatami, J. Am. Ceram. Soc. 82 (1999) 2993–2998.
[7] P.G. Zhang, K.Y. Wang, S.M. Guo, Ceram. Int. 36 (2010) 2209–2213.
[8] R.K. Paul, K.H. Lee, B.T. Lee, H.Y. Song, Mater. Chem. Phys. 112 (2008) 562–565.
[9] Y. Tang, H. Cong, Z. Wang, H.M. Cheng, Chem. Phys. Lett. 416 (2005) 171–175.
[10] S.C. Shi, S. Chattopadhyay, C.F. Chen, K.H. Chen, L.C. Chen, Chem. Phys. Lett. 418 (2006) 152–157.
[11] D.G. Zhao, J.J. Zhu, D.S. Jiang, H. Yang, J.W. Liang, X.Y. Li, H.M. Gong, J. Cryst. Growth 289 (2006) 72–75.
[12] Y. Mori, Y. Sugahara, Nippon. Seram. Kyo. Gak. 114 (2006) 461–472.
[13] K. Sardar, C.N.R. Rao, Solid State Sci. 7 (2005) 217–220.
[14] M. Radwan, Y. Miyamoto, J. Am. Ceram. Soc. 90 (2007) 2347–2351.
[15] A. Calka, J.I. Nikolov, Nanostruct. Mater. 6 (1995) 409–412.
[16] P. Li, S. Xi, J. Zhou, Ceram. Int. 35 (2009) 247–251.
[17] S.L. James, C.J. Adams, C. Bolm, D. Braga, P. Collier, T. Friić, F. Grepioni, K.D.M. Harris, G. Hyett, W. Jones, A. Krebs, J. MacK, L. Maini, A.G. Orpen, I.P. Parkin, W.C. Shearouse, J.W. Steed, D.C. Waddell, Chem. Soc. Rev. 41 (2012) 413–447.
[18] Y. Kameshima, M. Irie, A. Yasumori, K. Okada, Solid State Ionics 172 (2004) 185–190.
[19] S. Xi, X. Liu, P. Li, J. Zhou, J. Alloys Compd. 457 (2008) 452–456.
[20] J. Cintas, J.M. Montes, F.G. Cuevas, E.J. Herrera, J. Alloys Compd. 458 (2008) 282–285.
[21] Y. Du, M. Lei, H. Yang, J. Mater. Sci. Technol. 24 (2008) 737–741.
[22] M. Lei, H.Z. Zhao, H. Yang, B. Song, L.Z. Cao, P.G. Li, W.H. Tang, J. Alloys Compd. 460 (2008) 130–137.
[23] H. Zhao, M. Lei, X. Chen, W. Tang, J. Mater. Chem. 16 (2006) 4407–4412.
[24] H. Zhao, M. Lei, X. Yang, J. Jian, X. Chen, J. Am. Chem. Soc. 127 (2005) 15722–15723.
[25] W. Zhang, Z. Li, D. Zhang, J. Mater. Res. 25 (2010) 464–470.
[26] S.A. Rounaghi, A.R. Kiani-Rashid, H. Eshghi, J. Vahdati-Khaki, J. Solid State Chem. 190 (2012) 8–11.
[27] H.D. Li, G.T. Zou, H. Wang, H.B. Yang, D.M. Li, M.H. Li, S. Yu, Y. Wu, Z.F. Meng, J. Phys. Chem. B 102 (1998) 8692–8695.
[28] I. Ganesh, N. Thiyagarajan, G. Sundararajan, S.M. Olhero, J.M.F. Ferreira, J. Eur. Ceram. Soc. 28 (2008) 2281–2288.
[29] Q. Wu, Z. Hu, XZ. Wang, Y.N. Lu, X. Chen, H. Xu, Y. Chen, J. Am. Chem. Soc. 125 (2003) 10176–10178.
[30] C. Liu, Z. Hu, Q. Wu, X.Z. Wang, Y. Chen, H. Sang, J.M. Zhu, S.Z. Deng, N.S. Xu, J. Am. Chem. Soc. 127 (2005) 1318–1322.
[31] M. Kawaguchi, T. Yamanaka, Y. Hayashi, H. Oda, J. Electrochem. Soc. 157 (2010) A35–A40.
[32] M. Kawaguchi, A. Itoh, S. Yagi, H. Oda, J. Power Sources 172 (2007) 481–486.
[33] S. Matsumoto, K.K. Chattopadhyay, M. Mieno, T. Ando, J. Mater. Res. 13 (1998) 180–186.
[34] J.H. Kaufman, S. Metin, D.D. Saperstein, Phys. Rev. B 39 (1989) 13053–13060.
[35] F.A. Cotton, G. Wilkinson, C.A. Murillo, M. Bochmann, Advanced Inorganic Chemistry, 6th ed., Wiley, New York, 2000.